Evaluation of 3D-human skin equivalents for assessment of human dermal absorption of some brominated flame retardants

Abdallah, Mohamed; Pawar, Gopal; Harrad, Stuart

DOI:
10.1016/j.envint.2015.07.015

Document Version
Peer reviewed version

Citation for published version (Harvard):
Abdallah, M, Pawar, G & Harrad, S 2015, 'Evaluation of 3D-human skin equivalents for assessment of human dermal absorption of some brominated flame retardants', *Environment International*, vol. 84, pp. 64-70. https://doi.org/10.1016/j.envint.2015.07.015

EVALUATION OF 3D-HUMAN SKIN EQUIVALENTS FOR ASSESSMENT OF HUMAN DERMAL ABSORPTION OF SOME BROMINATED FLAME RETARDANTS

Mohamed Abou-Elwafa Abdallah[1,2*], Gopal Pawar[1] and Stuart Harrad[1]

[1]Division of Environmental Health and Risk Management,
College of Life and Environmental Sciences,
University of Birmingham,
Birmingham, B15 2TT,
United Kingdom.

[2]Department of Analytical Chemistry
Faculty of Pharmacy, Assiut University
71526 Assiut,
Egypt

* Corresponding author
Email mae_abdallah@yahoo.co.uk
Tel. +44121 414 7297
Fax. +44121 414 3078

Abstract

Ethical and technical difficulties inherent to studies in human tissues are impeding assessment of the dermal bioavailability of brominated flame retardants (BFRs). This is further complicated by increasing restrictions on the use of animals in toxicity testing, and the uncertainties associated with extrapolating data from animal studies to humans due to inter-species variations. To overcome these difficulties, we evaluate 3D-human skin equivalents (3D-HSE) as a novel *in vitro* alternative to human and animal testing for assessment of dermal absorption of BFRs. The percutaneous penetration of hexabromocyclododecanes (HBCD) and tetrabromobisphenol-A (TBBP-A) through two commercially available 3D-HSE models was studied and compared to data obtained for human *ex vivo* skin according to a standard protocol. No statistically significant differences were observed between the results obtained using 3D-HSE and human *ex vivo* skin at two exposure levels. The absorbed dose was low (less than 7%) and was significantly correlated with log K_{ow} of the tested BFR. Permeability coefficient values showed increasing dermal resistance to the penetration of γ-HBCD > β-HBCD > α-HBCD > TBBPA. The estimated long lag times (> 30 minutes) suggests that frequent hand washing may reduce human exposure to HBCDs and TBBPA via dermal contact.

Keywords: Dermal absorption, Human skin equivalents, Human *ex vivo* skin, HBCDs, TBBPA, EPISKIN.

47 **Introduction**

48 Brominated flame retardants (BFRs) are a diverse group of chemicals widely used to prevent
49 or reduce the flammability and combustibility of polymers and textiles. Among the major
50 members of this group are Tetrabromobisphenol A (TBBP-A) and hexabromocyclododecane
51 (HBCD) with estimated global production volumes of 170,000 and 16,700 tons, respectively
52 (BSEF 2014). Since HBCD and ~20% of the produced TBBP-A are blended physically
53 within, rather than bound chemically to polymeric materials; they migrate from products,
54 following which their persistence and bioaccumulative character leads to contamination of
55 the environment including humans (Harrad, et al. 2010). This is of concern owing to their
56 potential toxicological risks including: endocrine disruption, neurodevelopmental and
57 behavioral disorders, hepatotoxicity and possibly cancer (Darnerud 2008; Wikoff and
58 Birnbaum 2011). Such evidence has contributed to several regulations (e.g. REACH) under
59 different jurisdictions to control the production and use of these hazardous chemicals.
60 Recently, HBCD was listed under Annex A of the Stockholm Convention on Persistent
61 Organic Pollutants (POPs) (UNEP 2014).

62 Substantial data exist on concentrations of different FRs in various environmental and human
63 matrices (Covaci, et al. 2009; Law, et al. 2014; van der Veen and de Boer 2012). Current
64 understanding is that non-occupational human exposure to BFRs occurs mainly via a
65 combination of diet, ingestion of indoor dust, dermal contact with dust/consumer products,
66 and inhalation of indoor air (Abdallah, et al. 2008a; Frederiksen, et al. 2009; Watkins, et al.
67 2011). The exact contribution of these pathways varies substantially between chemicals,
68 between individuals according to lifestyle, and is further complicated by international
69 variations in FR use (Abdallah and Harrad 2009; Abdallah, et al. 2008a; Abdallah, et al.
70 2008b).

71 Currently, very little is known about dermal uptake as a route of human exposure to BFRs in

indoor dust or flame-retarded products. Watkins et al. reported a significant positive correlation between PBDE levels on hand wipes (presumably resulting from hand contact with contaminated dust or flame-retarded products) and PBDE levels in blood serum from American adults. While concentrations of PBDEs in indoor dust were strongly correlated with those in hand wipes, correlation could not be established directly between PBDE concentrations in indoor dust and their levels in serum (Watkins, et al. 2011). This opens up the possibility that FRs in dust may also be an indicator of another exposure pathway, such as direct dermal uptake of FRs present in treated goods (e.g. games consoles, remote controls, and fabrics). However, the absence of experimental data on human dermal absorption of various BFRs was recently highlighted as a major research gap hampering their accurate exposure assessment. Efforts to fill this gap are currently impeded by several difficulties including: ethical and technical issues inherent to studies involving human tissues, increasing restrictions on the use of laboratory animals in toxicological studies and the substantial uncertainties associated with extrapolating data from animal studies to humans due to inter-species variation (e.g. skin barrier function, hair follicles, intercellular subcutaneous lipids …etc) (Abdallah, et al. 2015a).

To overcome these difficulties, this study will evaluate the application of *in vitro* 3D-human skin equivalents (3D-HSE) as an alternative method to animal and human testing for assessment of dermal uptake of HBCDs and TBBPA. 3D-HSE are commercially available, fully differentiated, multi-layered dermal tissues that closely mimic the original human skin histologically and physiologically (Schaefer-Korting, et al. 2008a). 3D-HSE consist mainly of primary human cells (e.g. keratinocytes and fibroblasts) obtained from healthy consenting donors, which are then cultured at the air-liquid interphase on a specially designed inert support that allows cell growth in a nutrient culture medium (Figure SI-1). While cells grown in 2D monolayers (e.g. Caco-2 cell models) cannot capture the relevant complexity of the *in*

97 *vivo* microenvironment as they lack a myriad of important signals, key regulators, and tissue
98 phenotypes; cells growing in 3D tissue cultures have different cell surface receptor
99 expression, proliferative capacity, extracellular matrix synthesis, cell density, and metabolic
100 functions that resemble closely the original human tissue (Brohem, et al. 2011).
101 Consequently, validated protocols using 3D-HSE models have been approved by the OECD
102 (Organisation for Economic Co-operation and Development) and ECVAM (European Centre
103 for Validation of Alternative Methods) for testing skin irritation, phototoxicity and corrosion
104 by xenobiotic chemicals (Ackermann, et al. 2010; Buist, et al. 2010).
105 While 3D-HSE have been successfully applied within the cosmetics and pharmaceutical
106 sectors to study dermal uptake of various drugs (Ackermann, et al. 2010; Schaefer-Korting, et
107 al. 2008a), this study of dermal uptake of BFRs, is the first application of 3D-HSE to better
108 understanding of human dermal uptake of environmental contaminants. Our overall objective
109 was to demonstrate the substantial potential of these models to transform how human dermal
110 exposure to such contaminants is assessed. Nested within this, our specific aims were to: (a)
111 develop and apply a standard protocol for assessment of percutaneous penetration of HBCDs
112 and TBBPA using 2 commercially available 3D-HSE models (EPISKIN™ and EpiDerm™)
113 according to the OECD guidelines; (b) compare the results of 3D-HSE models to those
114 obtained from *in vitro* excised human skin (*ex vivo* skin); and (c) provide the first insights
115 into the dermal bioavailability of our target BFRs in humans.
116
117 **Materials and Methods**
118 Experiments were performed along the principles of good laboratory practice and in
119 compliance with the OECD guidelines for *in vitro* dermal absorption testing (OECD 2004).
120 The handling instructions and performance characteristics of the tested 3D-HSE models were
121 also taken into consideration. The study protocol received the required ethical approval *(#*

ERN_12-1502) from the University of Birmingham's Medical, Engineering and Mathematics Ethical Review Committee.

Test matrices.

The EpiDerm™ *EPI-212-X* human skin equivalent kit was purchased from MatTek Corporation (Ashland, MA). The *EPI-212-X* tissue constructs are 0.64 cm^2 human skin equivalents resembling the normal human epidermis histologically and physiologically (www.mattek.com). The kit includes maintenance medium (MM) - which is a proprietary DMEM (Dulbecco's Modified Eagle's Medium)-based medium - that allows acceptable differentiated morphology of the tissue for ~ 5 days upon receipt by end users.

The EPISKIN™ RHE/L/13 human skin equivalent kit was purchased from SkinEthic Laboratories (Lyon, France). The RHE/L/13 tissue constructs are 1.07 cm^2 supplied with enough MM to allow acceptable tissue differentiation (www.episkin.com). Upon receipt, the EPISKIN™ and EpiDerm™ tissues were equilibrated overnight with their MM at 5% CO_2 and 37 ˚C before use in the permeation experiments.

Fresh excised human upper breast skin was obtained via Caltag Medsystems Ltd. (Buckingham, UK) from 3 consented female adults (aged 36, 33 and 37 years) following plastic surgery. Selection criteria included: Caucasian, no stretchmarks, no scars and no hair. Full thickness skin without adipose tissue and an overall thickness of 550 ± 80 μm was used. Upon receipt, the *ex vivo* skin samples were equilibrated for 1 hour with 3 mL of DMEM-based (Sigma-Aldrich, UK) culture medium (Table SI-1) at 5% CO_2 and 37 ˚C before use in permeation experiments.

Dosing Solutions

According to the OECD guidelines (OECD 2004), two different concentration levels of (I) 5

147 ng/μL and (II) 10 ng/μL of each of α-HBCD, β-HBCD, γ-HBCD and TBBP-A (Wellington
148 Laboratories Inc., ON, Canada) were prepared in acetone. Based on the exposed surface area,
149 a net dose of 500 ng/cm^2 (~7.8 μM/cm^2) and 1000 ng/cm^2 (~15.6 μM/cm^2) was applied to
150 each of the investigated skin tissues using an appropriate volume (100 μL) of dosing
151 solutions I and II, respectively. The applied doses fall within the range of potential human
152 exposure to the studied BFRs via contact with indoor dust (Abdallah, et al. 2008a). Moreover,
153 they allow for measurement of expected low percentages (up to 0.01%) of the applied dose in
154 various compartments of the exposure model.
155 To study the possible effect of the dosing vehicle on the percutaneous penetration of the
156 tested chemicals, target BFRs were dissolved in 3 different dosing vehicles of: (A) acetone,
157 (B) 30% acetone in water, and (C) 20% Tween 80 (Sigma-Aldrich, UK) in water at a
158 concentration of 5 ng/μL. Preparation of the higher dosing level (i.e. 10 ng/μL) was not
159 possible due to limited solubility of target BFRs in vehicles (B) and (C).
160
161 *Permeation assay protocol*
162 The permeation experiments were performed using the static set-up approach (Figure 1). Skin
163 tissues were mounted in standard Franz-type permeation devices with *stratum corneum*
164 facing up. Based on the recommendation of the 3D-HSE providers, the EpiDerm™ tissues
165 were mounted in specifically designed MatTek™ permeation devices (MatTek Corporation,
166 Ashland, MA), the EPISKIN™ tissues were mounted in special inserts constructed for this
167 model (SkinEthic Laboratories, Lyon, France), while excised human skin tissues were
168 mounted in standard glass Franz cells.
169 All experiments were performed in triplicate. Following 30 minutes equilibration, the tested
170 chemicals were applied onto the skin surface in the donor compartment. A DMEM-based
171 culture medium (Table SI-1) was used as receptor fluid, maintained at 32 ± 1 °C and

172 magnetically stirred. To comply with the OECD guidelines, 5% bovine serum albumin (BSA)
173 was added to the receptor fluid (Table SI-1) to enhance the solubility of target analytes, while
174 the levels of test compounds in the donor solutions were chosen to ensure that the
175 concentrations in the receptor fluid during the experiment did not exceed 10% of the
176 saturation solubility.
177 At fixed time points (0.25, 0.5, 0.75, 1, 2, 4, 6, 10, 12, 18, 20 and 24 h), aliquots of the
178 receptor fluid (2 mL) were collected from the receptor compartment and immediately
179 replaced with fresh fluid. After 24 hours, the entire receptor fluid was collected and the skin
180 surface washed thoroughly with cotton buds impregnated in (1:1) hexane:ethyl acetate (5
181 times). The tissues were removed from the permeation devices and both the donor and
182 receptor compartments were washed separately (5 x 2 mL) with (1:1) hexane:ethyl acetate.
183 All samples were stored at -20 ˚C until chemical analysis.
184
185 *Sample extraction and chemical analysis*
186 Each permeation assay generated five different types of samples comprising: receptor fluid at
187 various time points, skin tissue, cotton buds (used to thoroughly wipe the skin surface), donor
188 and receptor compartment washes.
189 The receptor fluid, skin tissue and cotton bud samples were extracted according to a
190 previously reported QuEChERs-based method (Abdallah, et al. 2015b) (more details in the
191 supplementary data section).
192 The donor and receptor compartment washes were spiked with 30 ng of the ^{13}C-labeled
193 internal standard mixture prior to direct evaporation under a gentle stream of N_2. Target
194 analytes were reconstituted in 100 µL of methanol containing 100 pg/µL d_{18}- α-HBCD used
195 as recovery determination (syringe) standard for QA/QC purposes.
196 Instrumental analysis was carried out using an LC-MS/MS system composed of a dual pump

197 Shimadzu LC-20AB Prominence liquid chromatograph equipped with SIL-20A autosampler,
198 a DGU-20A3 vacuum degasser coupled to a Sciex API 2000 triple quadrupole mass
199 spectrometer. Details of the multi-residue analytical methodology used for separation and
200 quantification of the studied BFRs can be found elsewhere (Abdallah and Harrad 2011), with
201 a brief description provided as supplementary data.
202
203 *Data analysis and statistical methods*
204 A quantitative description of test compound permeation through the skin barrier is obtained
205 from Fick's first law of diffusion as follows (Niedorf, et al. 2008):

$$J_{ss} = \frac{\Delta m}{\Delta t . A} = \frac{D . K . \Delta C}{\Delta x} \qquad (1)$$

206 Where J_{ss} = steady-state flux [ng/cm^2.h]; Δm = permeated mass [ng]; Δt = time interval [h]; D
207 = diffusion coefficient [cm^2/h]; K = partition coefficient; A = area [cm^2]; Δc = concentration
208 difference [ng/cm^3]; Δx: thickness of membrane [cm].
209 When using infinite-dose configurations, i.e. in which the donor concentration far exceeds the
210 concentration in the receptor compartment ($C_D >> C_A$), ΔC can be replaced by the known
211 donor concentration, C_D, and the permeated mass per time assumed constant. Therefore, the
212 apparent permeation coefficient (P_{app}), which represents an independent measure of the
213 membrane resistance against permeation of the examined substance, can be calculated as:

$$P_{app} = \frac{J_{ss}}{C_D} \qquad (2)$$

214 For each permeation experiment, cumulative amounts of the permeated compounds in the
215 receptor fluid per unit area (ng/cm^2) were plotted versus time (hours). Steady state conditions
216 were indicated by a linear regression line ($R^2 \geq 0.9$), the slope of which represents the flux
217 (J_{ss}). Determination of the start and upper boundary of the linear range (i.e. steady state
218 conditions) was achieved according to the method described by Niedorf et al. (Niedorf, et al.

2008) (a summary flow chart is provided in figure SI-2).

Results are presented as the arithmetic mean of 3 replicates ± standard deviation (SD). Statistical analysis was performed using SPSS 13.0 software package. Differences in skin permeation were evaluated by the paired student t-test between 2 datasets. A Games-Howell test was used for analysis of variance (ANOVA) among several datasets with equal variances not assumed; $p < 0.05$ was regarded to indicate a statistically significant difference.

QA/QC

Several stages of QA/QC measurements were performed to check the performance of permeation assay protocol. A "field" blank, comprising a skin tissue exposed to solvents only and treated as a sample, was performed with each sample batch (n= 9). None of the studied compounds were above the limit of detection (LOD) in the field blank samples. Good recoveries of the ^{13}C-labeled internal standards (> 80%) were obtained indicating high efficiency of the extraction method (Table SI-3).

Based on the guidelines of EPISKIN™ and EpiDerm™ models, the viability of the tissue was tested by MTT (3-(4,5-dimethylthiazol-2-yl)-2,5-diphenyltetrazolium bromide) assay using a standard kit purchased from each provider. Acceptable MTT results (i.e. Formazan concentration ≥ 1.5 mg/ml) were achieved following 24 hours of exposure. Both positive and negative control experiments were carried out alongside each sample batch. Positive controls involved the exposure of the test tissue to Triton-X-100 which showed ~ 100% permeation (n=5; 97 ± 4%), while negative controls showed 0% penetration of decabromodiphenyl ethane after 24 hours exposure. The integrity of the skin membrane was tested using the standard trans-epidermal electrical resistance (TEER) and methylene blue (BLUE) standard methods (Guth, et al. 2015). One excised human skin patch failed the membrane integrity test; hence its results were excluded from this study.

Results and Discussion

Mass balance and absorbed fractions

The efficiency of the experimental approach was investigated using a mass balance exercise. Results revealed good overall recoveries (>85%) for the target compounds using different permeation devices (Table 1). However, the use of specifically-designed permeation devices for the EPISKIN™ and EpiDerm™ models minimized the formation of air bubbles underneath the skin surface and reduced the handling-time and operator involvement during sampling of the receptor fluid at different time points.

For simplicity, results of the permeation experiments were grouped under three major compartments: The directly absorbed dose (cumulative concentration in the receptor fluid over 24 h + receptor compartment rinse), the skin (concentration in the skin tissue after 24 h) and the unabsorbed dose (concentration in the skin surface wipes after 24 h + donor compartment rinse). Experimental results revealed higher permeation of all target compounds in the following order: EpiDerm™ >EPISKIN™ > Human *ex vivo* skin at the two concentration levels studied (Table 1 and Table SI-4). However, statistical analysis showed no significant differences ($P > 0.05$) among the levels of target analytes in the 3 major compartments of the examined tissues. Border line statistical significances ($P = 0.053$ and 0.056) were observed between the results of human *ex vivo* skin and those of EpiDerm™ for β-HBCD and EPISKIN™ for TBBPA, respectively. The EpiDerm™ model displayed the largest permeation difference from human *ex vivo* skin with ~25% increase in the permeated dose of β-HBCD over 24 hours exposure.

Previous studies comparing percutaneous permeation of chemicals through different *in vitro* models reported substantial inter-model differences. A 7-fold higher flux was observed for 11 pesticides across *in vitro* rat skin compared to human skin (van Ravenzwaay and Leibold

2004). For triclosan, a 3-fold higher dermal absorption in rat compared to human skin was observed, while an 8-fold increase in the absorbed dose was reported for BDE-47 (Roper, et al. 2006). Mouse skin showed higher permeability to several chemicals, *in vitro*, than either rat, pig or human skin (Hughes, et al. 2001). A comparative study conducted in 2006 according to OECD guidelines reported less penetration of testosterone in pig and bovine skin (0.07 and 0.13 % of applied dose) compared to human skin (0.32 %), while EPISKIN™ and EpiDerm™ models showed higher permeations (0.53 and 2.36, respectively) (Schafer-Korting, et al. 2006). It is noteworthy that both 3D-HSE producers claim that their skin models were further developed since 2006 to improve the barrier function. Hence the EPISKIN™ and EpiDerm™ models used in this study are listed under the "enhanced barrier function" category, which is different from those used in the 2006 study. Another well-designed study reported higher diffusion of radiolabeled bisphenol A (BPA) through pig ear skin (65%) compared to human skin (45%), although the difference was not statistically significant at the 95% confidence level (Zalko, et al. 2011).

Investigation of the directly absorbed dose through the tested skin models showed a uniform pattern of increasing permeation in the following order: TBBP-A > α-HBCD > β-HBCD > γ-HBCD (Figure 2). This is generally in line with the physicochemical properties of the tested compounds, where TBBP-A has a lower mass and higher water solubility than HBCDs (Table SI-6). Furthermore, a statistically significant correlation ($P < 0.05$) was observed between the 24 h cumulative absorbed dose and the log K_{OW} (Table SI-6) of the studied BFRs in all the tested *in vitro* models. This highlights the influence of physicochemical properties on the human dermal bioavailability of a chemical.

Dermal flux ($\boldsymbol{J_{ss}}$) and permeation coefficients ($\boldsymbol{P_{app}}$)

A plot of the cumulative absorbed mass of each target compound (ng/cm^2) against time (hours) was used to estimate the J_{ss} (ng/cm^2.h) for each target BFR and the P_{app} (cm/h) for the examined skin models (Table 2). The steady state range of the curve was identified according to the method reported by Niedorf et al. (Niedorf, et al. 2008), with a minimum of 5 data points in the linear range required to establish each curve (Figure SI-3, Table SI-5).

Following the application of a test compound to the skin, it needs to partition into and diffuse through the skin before reaching the receptor fluid. This results in a lag-time, t_{lag}, with non-detectable flux. The t_{lag} is represented by the time intercept (i.e. x-axis intercept) of the regression line over the steady-state region of the permeation curve (Figure SI-3). Hence, t_{lag} can be calculated from equation 3:

$$t_{lag} = \frac{b_0}{J_{ss}} \ldots\ldots\ldots\ldots (3)$$

Where b_0 refers to the y-axis intercept of the linear regression line and J_{ss} is the slope.

Steady state flux (J_{ss}) provides quantitative description of a xenobiotic permeation through the dermal barrier. This is expressed as the rate (ng/ cm^2. h) by which the tested chemical traverses the skin tissue to reach the receptor fluid (Niedorf, et al. 2008). With γ-HBCD showing lowest percutaneous penetration and TBBPA the highest, J_{ss} of the studied BFRs ranged from 0.8 - 1.5 ng/ cm^2. h, 0.9 - 1.5 ng/ cm^2. h and 0.7 - 1.3 ng/ cm^2. h for the EPISKIN™, EpiDerm™ and human *ex vivo* skin, respectively (Table 2). Interestingly, α-HBCD showed a consistently higher flux across skin than γ-HBCD at the studied doses (Table 2). This indicates a higher dermal bioavailability of α-HBCD compared to the β- and γ- isomers. In addition to slower biotransformation rates (Abdallah, et al. 2014) and higher uptake from the gastrointestinal tract (Abdallah, et al. 2012), the greater dermal bioavailability of α-HBCD is likely a contributory factor in the dramatic shift of the HBCD isomeric profile from predominantly γ-HBCD in the commercial formulations and abiotic samples to a predominance of α-HBCD in biota (Covaci, et al. 2006).

317 The estimated P_{app} values indicate more resistance of human *ex vivo* skin to the penetration of
318 target BFRs than the EPISKIN™ and EpiDerm™ models. However, this difference was not
319 statistically significant. In addition, both 3D-HSE models and human *ex vivo* skin displayed
320 increasing resistance to the penetration of BFRs in the same order of γ-HBCD > β-HBCD >
321 α-HBCD > TBBP-A.
322 The lipophilic nature, low polarity and low water solubility of the studied BFRs are
323 manifested by long lag times (> 30 minutes; Table 2), which suggests that frequent hand
324 washing may reduce human exposure to HBCDs and TBBPA via dermal contact. This is
325 generally in line with the results of Watkins et al. who found that adults washing their hands
326 fewer than four times/day had, on average, 3.3 times more pentaBDE in their handwipes
327 compared with those who washed their hands four or more times/day and concluded that
328 frequent hand washing may decrease exposure to PBDEs via dermal contact (Watkins, et al.
329 2011).
330
331 *Effect of dosing vehicle*
332 Several studies in the pharmaceutical and cosmetic sectors have highlighted the influence of
333 dosing vehicle on the percutaneous penetration of chemicals. However, these experiments
334 were exclusively based on aqueous solutions and topical emulsions (Schaefer-Korting, et al.
335 2008b). Very little is known about the quantitative effects of organic-based vehicles on the
336 dermal penetration of xenobiotics. In general, a vehicle may hydrate the stratum corneum
337 (SC), extract critical barrier components out of the skin, or damage the skin because it is a
338 strong acid or base. Removing SC lipids may increase percutaneous absorption of drugs.
339 Many organic solvents (e.g. chloroform and methanol) are employed to delipidize the skin,
340 which increases the permeability of hydrophilic - but not lipophilic – compounds (Chiang, et
341 al. 2012).

342 Since BFRs are highly lipophilic compounds with very low water solubility (Table SI-6), the
343 few studies on their dermal absorption used organic vehicles to dissolve the target analytes.
344 Hughes et al. used tetrahydrofuran (THF) as a vehicle for BDE-209 (Hughes, et al. 2001),
345 while Roper et al. used acetone for dissolving BDE-47 (Roper, et al. 2006). In the current
346 study, acetone was selected as the major dosing vehicle. This was based on its ability to
347 dissolve the test compounds at the desired levels and its minimal effect on skin barrier
348 functions. Abrams et al. studied the effect of various organic solvents on the trans-epidermal
349 water loss (TEWL) as an indicator of skin barrier. Both acetone and hexane showed no
350 significantly different effects than water, while a mixture of chloroform : methanol (2:1)
351 caused the greatest significant increase in TEWL (Abrams, et al. 1993).
352 To further investigate the potential effect of the dosing vehicle on percutaneous penetration
353 of BFRs, human *ex vivo* skin and the EPISKIN™ model were exposed to 500 ng/cm^2 of
354 target BFRs in each of :(A) acetone, (B) 30% acetone in water, and (C) 20% Tween 80 in
355 water for 24 h. Results revealed higher levels of target compounds were absorbed from
356 vehicle C, which was more evident for TBBP-A and α-HBCD compared to β- and γ-HBCDs
357 (Figures 3 and SI-4). This is in agreement with the reported enhancement of the dermal
358 absorption of testosterone in the presence of surfactants including miglyol and Tween 80
359 (Schaefer-Korting, et al. 2008b).
360 Although the differences in permeation of the studied BFRs from the tested vehicles lacked
361 statistical significance, the enhanced permeation of TBBP-A and α-HBCD (Figure 3) in the
362 presence of Tween 80 is potentially pertinent within the context of human exposure. This is
363 owing to the presence of natural surface active agents in human skin surface film
364 (sweat/sebum mixture) (Stefaniak, et al. 2010), which may influence the dermal absorption of
365 these BFRs. Therefore, detailed study of the effect of human skin surface film on the dermal
366 uptake of various BFRs appears warranted in the near future. In conclusion, the data

367 presented here demonstrate the validity of the 3D-HSE models for studying human dermal
368 uptake of BFRs and related environmental contaminants.
369
370 **Acknowledgement**
371 The research leading to these results has received funding from the European Union Seventh
372 Framework Programme FP7/2007-2013 under grant agreements 327232 (ADAPT project)
373 and 316665 (A-TEAM project). Further support was provided by Restek Corporation.
374
375 **Supplementary data**
376 Further details of the analytical methodology, quality assurance/quality control parameters
377 and distribution of target BFRs in different compartments of the *in vitro* diffusion system are
378 available as supplementary data.
379
380
381
382
383
384
385
386
387
388
389
390
391

392 **References**

393 Abdallah, M.A.-E.; Harrad, S. Personal exposure to HBCDs and its degradation products via
394 ingestion of indoor dust. Environ Int. 35:870-876; 2009
395 Abdallah, M.A.-E.; Harrad, S. Tetrabromobisphenol-A, hexabromocyclododecane and its
396 degradation products in UK human milk: Relationship to external exposure. Environ Int.
397 37:443-448; 2011
398 Abdallah, M.A.; Harrad, S.; Covaci, A. Hexabromocyclododecanes and tetrabromobisphenol-
399 A in indoor air and dust in Birmingham, U.K: implications for human exposure. Environ
400 Sci Technol. 42:6855-6861; 2008a
401 Abdallah, M.A.; Uchea, C.; Chipman, J.K.; Harrad, S. Enantioselective Biotransformation of
402 Hexabromocyclododecane by in Vitro Rat and Trout Hepatic Sub-Cellular Fractions.
403 Environ Sci Technol. 48:2732-2740; 2014
404 Abdallah, M.A.E.; Harrad, S.; Ibarra, C.; Diamond, M.; Melymuk, L.; Robson, M., et al.
405 Hexabromocyclododecanes in indoor dust from Canada, the United Kingdom, and-the
406 United States. Environ Sci Technol. 42:459-464; 2008b
407 Abdallah, M.A.E.; Pawar, G.; Harrad, S. Evaluation of in vitro vs. in vivo methods for
408 assessment of dermal absorption of organic flame retardants: A review. Environ Int.
409 74:13-22; 2015a
410 Abdallah, M.A.E.; Tilston, E.; Harrad, S.; Collins, C. In vitro assessment of the
411 bioaccessibility of brominated flame retardants in indoor dust using a colon extended
412 model of the human gastrointestinal tract. J Environ Monitor. 14:3276-3283; 2012
413 Abdallah, M.A.E.; Zhang, J.K.; Pawar, G.; Viant, M.R.; Chipman, J.K.; D'Silva, K., et al.
414 High-resolution mass spectrometry provides novel insights into products of human
415 metabolism of organophosphate and brominated flame retardants. Anal Bioanal Chem.
416 407:1871-1883; 2015b

417 Abrams, K.; Harvell, J.D.; Shriner, D.; Wertz, P.; Maibach, H.; Maibach, H.I., et al. Effect of
418 organic-solvents on in-vitro human skin water barrier function. J Invest Dermatol.
419 101:609-613; 1993
420 Ackermann, K.; Borgia, S.L.; Korting, H.C.; Mewes, K.R.; Schafer-Korting, M. The Phenion
421 full-thickness skin model for percutaneous absorption testing. Skin Pharmacol Physiol.
422 23:105-112; 2010
423 Brohem, C.A.; da Silva Cardeal, L.B.; Tiago, M.; Soengas, M.S.; de Moraes Barros, S.B.;
424 Maria-Engler, S.S. Artificial skin in perspective: concepts and applications. Pigment Cell
425 & Melanoma Research. 24:35-50; 2011
426 BSEF. Bromine Science and Environmental Forum.www.bsef.com; 2014
427 Buist, H.E.; van Burgsteden, J.A.; Freidig, A.P.; Maas, W.J.; van de Sandt, J.J. New in vitro
428 dermal absorption database and the prediction of dermal absorption under finite conditions
429 for risk assessment purposes. Regul Toxicol Pharmacol. 57:200-209; 2010
430 Chiang, A.; Tudela, E.; Maibach, H.I. Percutaneous absorption in diseased skin: an overview.
431 J Appl Toxicol. 32:537-563; 2012
432 Covaci, A.; Gerecke, A.C.; Law, R.J.; Voorspoels, S.; Kohler, M.; Heeb, N.V., et al.
433 Hexabromocyclododecanes (HBCDs) in the environment and humans: a review. Environ
434 Sci Technol. 40:3679-3688; 2006
435 Covaci, A.; Voorspoels, S.; Abdallah, M.A.; Geens, T.; Harrad, S.; Law, R.J. Analytical and
436 environmental aspects of the flame retardant tetrabromobisphenol-A and its derivatives. J
437 Chromatogr A. 1216:346-363; 2009
438 Darnerud, P.O. Brominated flame retardants as possible endocrine disrupters. Int J Androl.
439 31:152-160; 2008

Frederiksen, M.; Vorkamp, K.; Thomsen, M.; Knudsen, L.E. Human internal and external exposure to PBDEs--a review of levels and sources. Int J Hyg Environ Health. 212:109-134; 2009

Guth, K.; Schaefer-Korting, M.; Fabian, E.; Landsiedel, R.; van Ravenzwaay, B. Suitability of skin integrity tests for dermal absorption studies in vitro. Toxicol in Vitro. 29:113-123; 2015

Harrad, S.; de Wit, C.A.; Abdallah, M.A.; Bergh, C.; Bjorklund, J.A.; Covaci, A., et al. Indoor Contamination with Hexabromocyclododecanes, Polybrominated Diphenyl Ethers, and Perfluoroalkyl Compounds: An Important Exposure Pathway for People? Environ Sci Technol. 44:3221-3231; 2010

Hughes, M.F.; Edwards, B.C.; Mitchell, C.T.; Bhooshan, B. In vitro dermal absorption of flame retardant chemicals. Food Chem Toxicol. 39:1263-1270; 2001

Law, R.J.; Covaci, A.; Harrad, S.; Herzke, D.; Abdallah, M.A.E.; Fernie, K., et al. Levels and trends of PBDEs and HBCDs in the global environment: Status at the end of 2012. Environ Int. 65:147-158; 2014

Niedorf, F.; Schmidt, E.; Kietzmann, M. The automated, accurate and reproducible determination of steady-state permeation parameters from percutaneous permeation data. Alternatives to laboratory animals : ATLA. 36:201-213; 2008

OECD. Guideline for the testing of chemicals. Skin absorption: in vitro method. Organisation for Economic Cooperation and Development TG 428; 2004

Roper, C.S.; Simpson, A.G.; Madden, S.; Serex, T.L.; Biesemeier, J.A. Absorption of C-14 - tetrabromodiphenyl ether (TeBDE) through human and rat skin in vitro. Drug Chem Toxicol. 29:289-301; 2006

Schaefer-Korting, M.; Bock, U.; Diembeck, W.; Duesing, H.-J.; Gamer, A.; Haltner-Ukomadu, E., et al. The use of reconstructed human epidermis for skin absorption testing:

results of the validation study. Alternatives to laboratory animals : ATLA. 36:161-187; 2008a

Schaefer-Korting, M.; Mahmoud, A.; Borgia, S.L.; Brueggener, B.; Kleuser, B.; Schreiber, S., et al. Reconstructed epidermis and full-thickness skin for absorption testing: Influence of the vehicles used on steroid permeation. Alternatives to laboratory animals : ATLA. 36:441-452; 2008b

Schafer-Korting, M.; Bock, U.; Gamer, A.; Haberland, A.; Haltner-Ukomadu, E.; Kaca, M., et al. Reconstructed human epidermis for skin absorption testing: results of the German prevalidation study. Alternatives to laboratory animals : ATLA. 34:283-294; 2006

Stefaniak, A.B.; Harvey, C.J.; Wertz, P.W. Formulation and stability of a novel artificial sebum under conditions of storage and use. International journal of cosmetic science. 32:347-355; 2010

UNEP. United Nations Environment Programme, Persistent Organic Pollutants Review Committee (POPRC), Reports and Decisions. http://chmpopsint/TheConvention/POPsReviewCommittee/OverviewandMandate/tabid/2806/Defaultaspx; 2014

van der Veen, I.; de Boer, J. Phosphorus flame retardants: Properties, production, environmental occurrence, toxicity and analysis. Chemosphere. 88:1119-1153; 2012

van Ravenzwaay, B.; Leibold, E. The significance of in vitro rat skin absorption studies to human risk assessment. Toxicol in Vitro. 18:219-225; 2004

Watkins, D.J.; McClean, M.D.; Fraser, A.J.; Weinberg, J.; Stapleton, H.M.; Sjoedin, A., et al. Exposure to PBDEs in the Office Environment: Evaluating the Relationships Between Dust, Handwipes, and Serum. Environ Health Persp. 119:1247-1252; 2011

Wikoff, D.S.; Birnbaum, L. Human Health Effects of Brominated Flame Retardants. In: Eljarrat EBD, ed. Handb Environ Chem; 2011

490 Zalko, D.; Jacques, C.; Duplan, H.; Bruel, S.; Perdu, E. Viable skin efficiently absorbs and
491 metabolizes bisphenol A. Chemosphere. 82:424-430; 2011

492

Tables

Table 1: Distribution of target BFRs (expressed as % of exposure dose) in different fractions of the *in vitro* diffusion system following 24 hour exposure to 500 ng/cm^2 of α-, β-, γ-HBCDs and TBBP-A in acetone.

	α-HBCD	β-HBCD	γ-HBCD	TBBP-A
	EPISKIN™			
Receptor fluid (24h)	5.81 ± 1.04	3.86 ± 0.78	3.42 ± 0.94	6.29 ± 0.65
Receptor rinse	0.10 ± 0.02	0.07 ± 0.02	0.11 ± 0.02	0.41 ± 0.28
Directly absorbed fraction	5.90 ± 1.06	3.94 ± 0.82	3.46 ± 0.96	6.70 ± 0.92
Skin-Epidermis (Depot)	30.06 ± 2.42	27.18 ± 2.28	23.66 ± 3.16	24.18 ± 2.54
Skin wash (unabsorbed)	44.34 ± 4.04	51.47 ± 3.72	56.82 ± 4.58	53.53 ± 3.46
Donor rinse (unabsorbed)	5.13 ± 0.64	3.16 ± 0.82	2.38 ± 1.06	4.93 ± 2.08
Unabsorbed dose	49.47 ± 4.68	54.63 ± 4.54	59.20 ± 5.64	58.46 ± 5.54
Total Recovery	85.43 ± 8.16	85.75 ± 7.64	86.32 ± 9.76	89.34 ± 9.02
	EpiDerm™			
Receptor fluid (24h)	6.35 ± 0.92	4.02 ± 1.04	3.74 ± 0.82	6.44 ± 0.59
Receptor rinse	0.11 ± 0.04	0.10 ± 0.08	0.09 ± 0.04	0.34 ± 0.16
Directly absorbed fraction	6.46 ± 0.94	4.13 ± 1.12	3.82 ± 0.86	6.78 ± 0.74
Skin-Epidermis (Depot)	28.19 ± 3.18	24.39 ± 2.22	21.02 ± 3.52	23.79 ± 2.42
Skin wash (unabsorbed)	45.73 ± 4.02	53.91 ± 3.44	58.84 ± 4.38	55.04 ± 4.29
Donor rinse (unabsorbed)	5.07 ± 0.62	2.39 ± 0.52	1.97 ± 0.74	4.11 ± 1.27
Unabsorbed dose	50.80 ± 4.64	56.30 ± 3.96	60.81 ± 5.12	59.15 ± 5.56
Total Recovery	85.45 ± 8.76	84.82 ± 7.30	85.65 ± 9.50	89.72 ± 8.72
	Human *ex vivo* skin			
Receptor fluid (24h)	4.88 ± 1.44	3.21 ± 1.06	3.01 ± 1.02	5.37 ± 0.65
Receptor rinse	0.07 ± 0.02	0.11 ± 0.02	0.06 ± 0.02	0.21 ± 0.28
Directly absorbed fraction	4.95 ± 1.44	3.32 ± 1.06	3.07 ± 1.48	5.57 ± 0.92
Skin-Epidermis (Depot)	30.59 ± 2.28	27.82 ± 2.38	24.16 ± 2.24	24.71 ± 2.96
Skin wash (unabsorbed)	47.05 ± 4.44	51.19 ± 4.68	56.48 ± 3.28	56.53 ± 4.46
Donor rinse (unabsorbed)	5.23 ± 1.48	3.37 ± 1.02	2.07 ± 0.66	3.83 ± 2.08
Unabsorbed dose	52.28 ± 5.92	54.56 ± 5.70	58.55 ± 3.94	60.37 ± 6.54
Total Recovery	87.82 ± 7.84	85.70 ± 6.28	85.78 ± 7.38	85.65 ± 10.42

Table 2: Steady state flux, permeation coefficient and lag time values estimated for the target BFRs using different *in vitro* skin models.

	Flux (J_{ss}) ($ng/cm^2.h$)	Permeation coefficient (P_{app}) (cm/h)	Lag time (h)
EPISKIN™			
α-HBCD	1.25	2.50×10^{-04}	0.80
β-HBCD	0.84	1.69×10^{-04}	1.01
γ-HBCD	0.78	1.56×10^{-04}	1.21
TBBPA	1.47	2.93×10^{-03}	0.72
EpiDerm™			
α-HBCD	1.33	2.74×10^{-04}	0.77
β-HBCD	0.88	1.77×10^{-04}	0.97
γ-HBCD	0.85	1.72×10^{-04}	1.13
TBBPA	1.48	2.97×10^{-03}	0.60
Human *ex vivo* skin			
α-HBCD	1.08	2.16×10^{-04}	0.85
β-HBCD	0.74	1.47×10^{-04}	1.17
γ-HBCD	0.69	1.37×10^{-04}	1.26
TBBPA	1.29	2.58×10^{-03}	0.79

Figures

Figure 1: General outline of the experimental protocol applied for percutaneous permeation experiments.

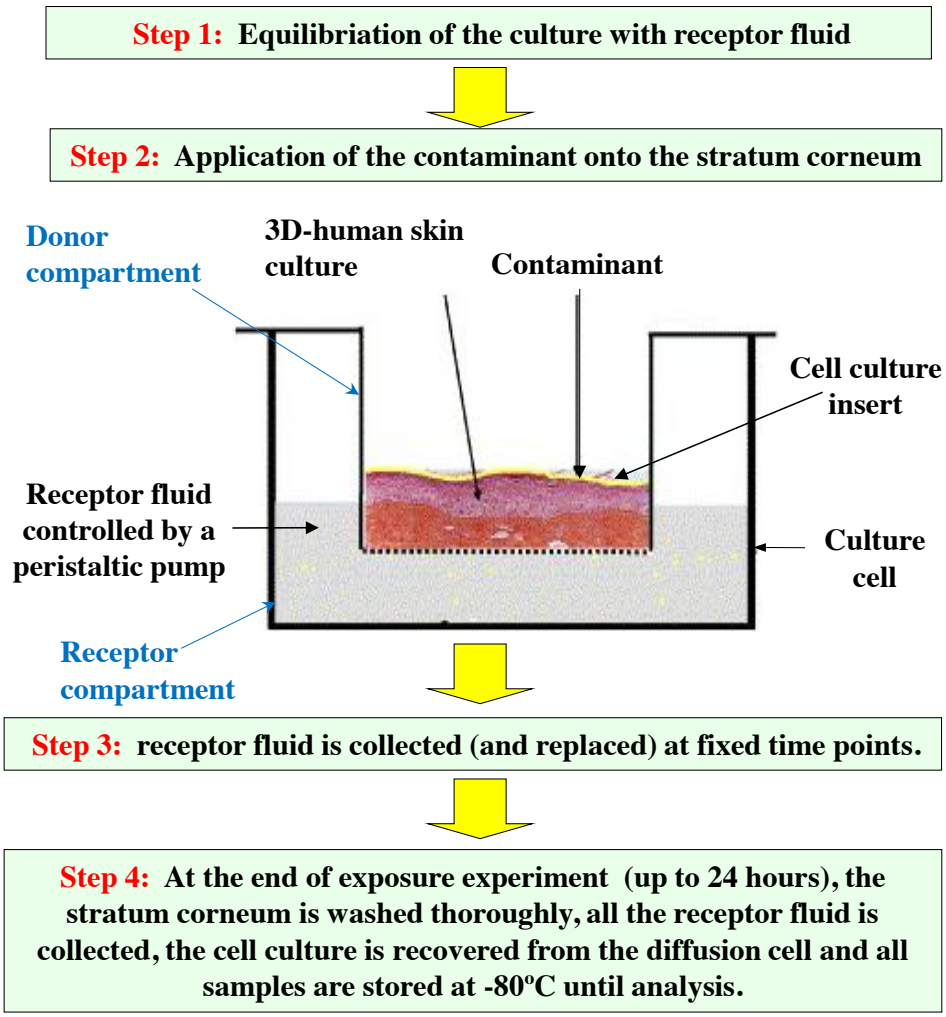

Figure 2: Cumulative dose absorbed into the receptor fluid following exposure of (a) human *ex vivo* skin, (b) EPISKIN™ and (c) EpiDerm™ to 1000 ng/cm^2 of target BFRs over 24 h.

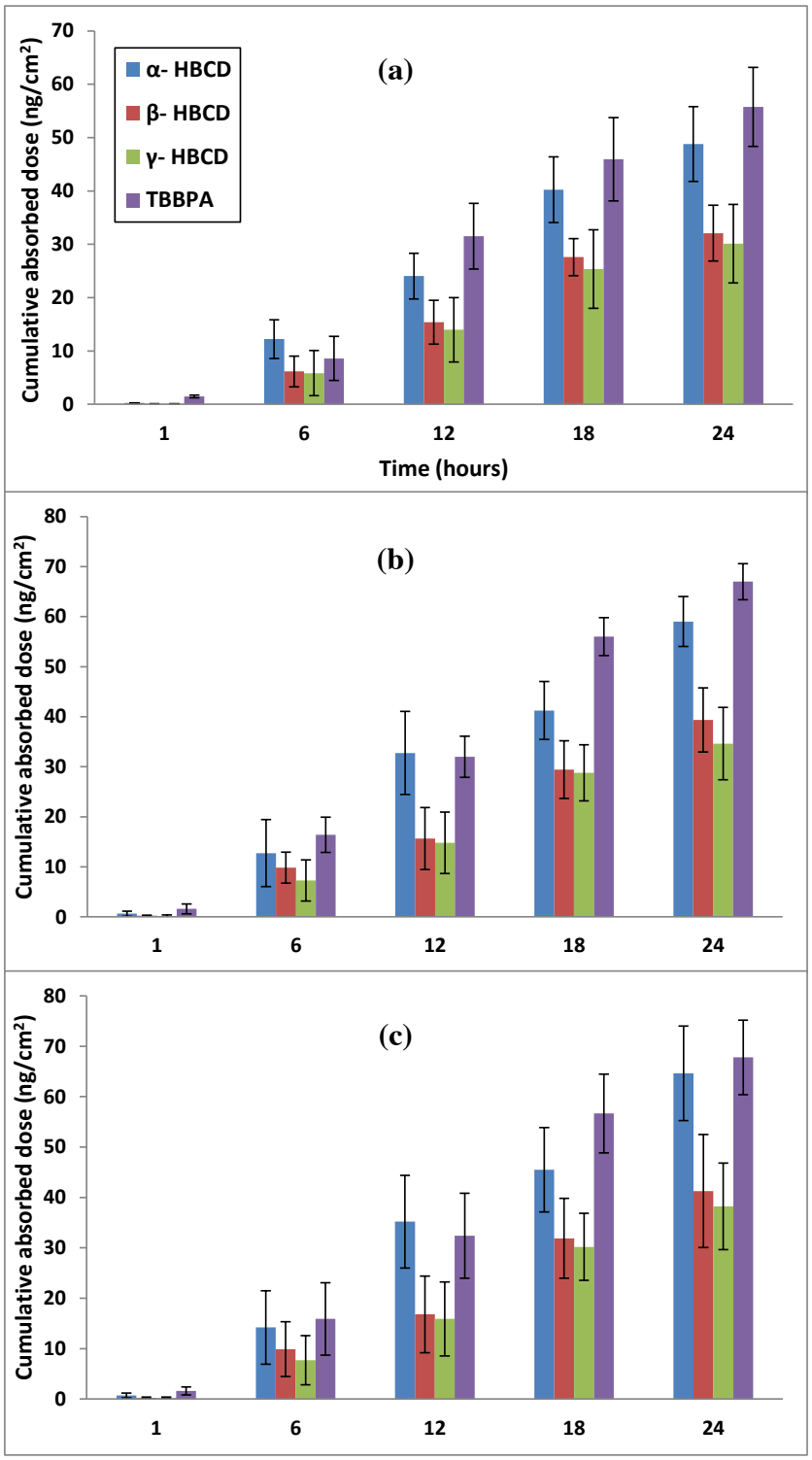

532 Figure 3: Cumulative permeation (ng/cm^2) into the receptor fluid following exposure of
533 EPISKIN™ model to 500 ng/cm^2 of target BFRs in (A) acetone, (B) 30% acetone in water,
534 and (C) 20% Tween 80 in water for 24 h.

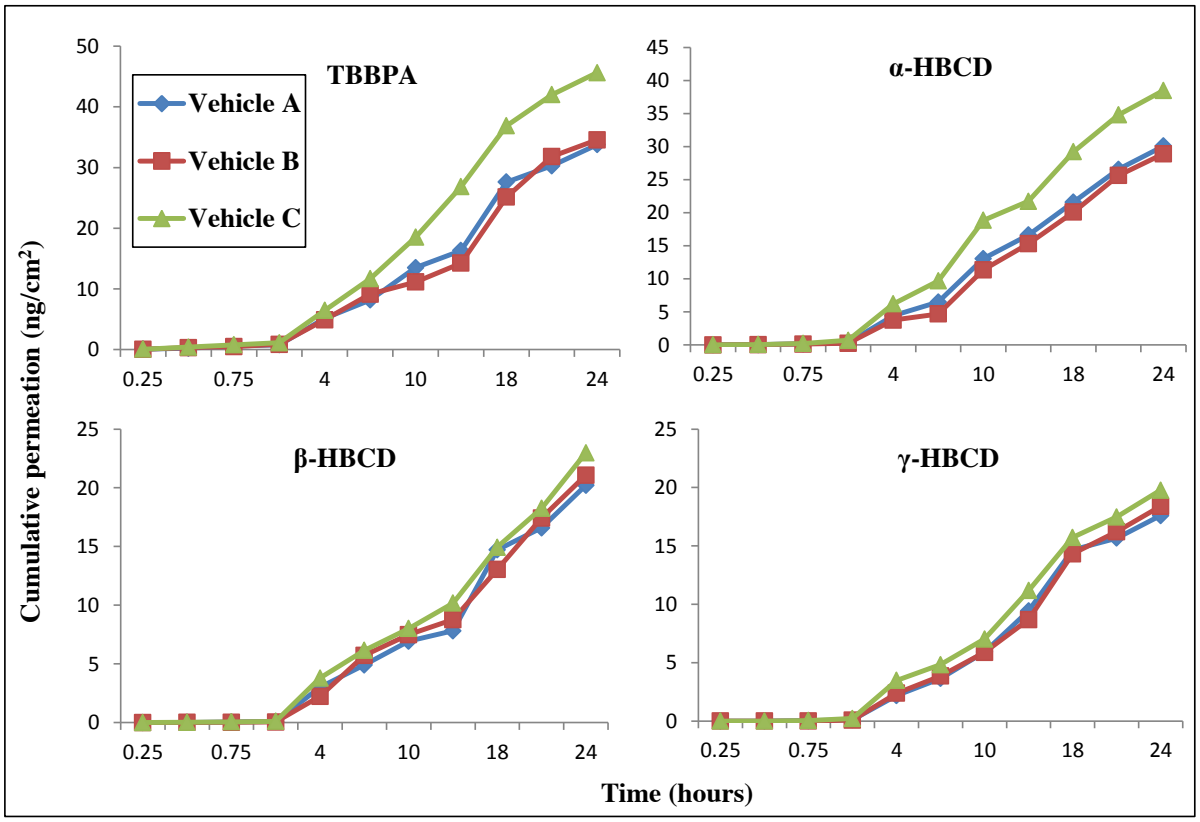

535

536

Supplementary Information

Click here to download Supplementary Information: SI_Abdallah et al 2015_R1_NFC.docx

Graphical Abstract